

In comparison to the minimum human water requirement estimated by Gleick (2005) of 50 litres per person per day for the activities of drinking, cooking, washing and sanitation the consumption at SANAE IV is more than 160 % higher. Calculated at 80 litres per person per day this figure is derived from documentation at the base suggesting that peak total daily takeover consumption amounts to 8000 litres (for the entire base of 80 people) while yearly averages of daily consumption range between 600 and 1000, or sometimes 2000 litres per day (for the overwintering team of 10).

Historically there has never been sufficient water available during the takeover periods. From the start of the takeover occupants are limited to showering every alternate day, with periods of total bans and other restrictions often implemented. Although attending continuously to the snow smelter would ensure a sufficient supply of water for all occupants and their activities this commodity does not come without a price. Part of the cost of producing this water is a considerable 95 kW spike in the electricity load at a time when the generators are experiencing difficulty in shedding heat and should ideally be producing less (Cencelli, 2002). An indication of the minimum amount of energy required to meet the average domestic takeover water demand is provided in table 3.1.

Table 3.1: Energy requirements of takeover water demand

PARAMETER	VALUE
Initial snow temperature (°C)	0
Final water temperature (°C)	30
Latent heat of fusion for snow (kJ/kg)	335
Cp of water (kJ/kg. K)	4.190
Average water requirement per person per day (litres)	80
Number of people	80
Minimum amount of energy required to melt the snow (kWh)	819
Equivalent minimum average daily electricity demand (kW)	34

The snow smelter is an energy intensive load where it makes sense to supplement the current demand with solar alternatives. This opportunity for use with solar energy devices is brought about mainly by the size of the load and its match with the availability of sunshine. It is also a thermal load, presenting the possible advantage of capturing energy at higher collector efficiencies than solar electric devices can deliver.

### 3.2.3 Heating and Ventilation System

A more thorough study of the Heating and Ventilation System (H&V System) is provided in appendix C.1. As explained in section 3.2.2, however, it is evident that the H&V System is 180 degrees “out of phase” with the availability of sunshine. During the summer there is ample heat available from the generators to keep the base warm (in fact it is necessary to cool the base) while conversely the winter periods are characterised by cold inside temperatures. With the obvious lack of sunshine during the winter periods it is evident that the Heating and Ventilation System is not an ideal application for the utilisation of solar energy. Nonetheless, as discussed in the appendix improving the current computer simulation programme of the station could indirectly result in significant savings.

### 3.2.4 Power Generation System

Central to all the operating systems are three ADE diesel-electric generators (viz. two turbo-charged ADE 442T with a rated power of 260 kW and one turbo-charged inter-cooled 442Ti rated at 320 kW) that output energy to the station’s electrical mini-grid at 3-phase, 380 VAC and 50 Hz. These generators are used on a rotational and load-sharing basis with only a single master generator operational while the electricity demand remains below 162 kW. A stand-by generator is always primed and ready for use should the load exceed this limit at which time load sharing occurs between the master and slave generators while the third generator is always left out of operation. This slave generator will only be switched off again when the demand drops to below 140 kW.

A number of corresponding electricity-production and diesel-consumption data points were collected for analysis (see appendix C.6). Consequently, it was found that the electrical efficiency of the generators is 36.4 %, although it is still uncertain what the combined thermal and electrical efficiency is. A useful and improved (from Teetz [2002]) linear regression correlation for the production of energy is given in equation 3.1, where total electrical energy production is calculated from generator diesel consumption using:

$$PP = 3.5652 \cdot FC - 2.5683 \quad 3.1$$

In this equation  $PP$  is power production in kWh,  $FC$  is diesel consumption in litres and the regression coefficient for the correlation is 0.99. Using equation 3.1, data from Teetz (2002) and

the fuel consumption data presented in section 3.3, some important parameters are derived and presented in table 3.2.

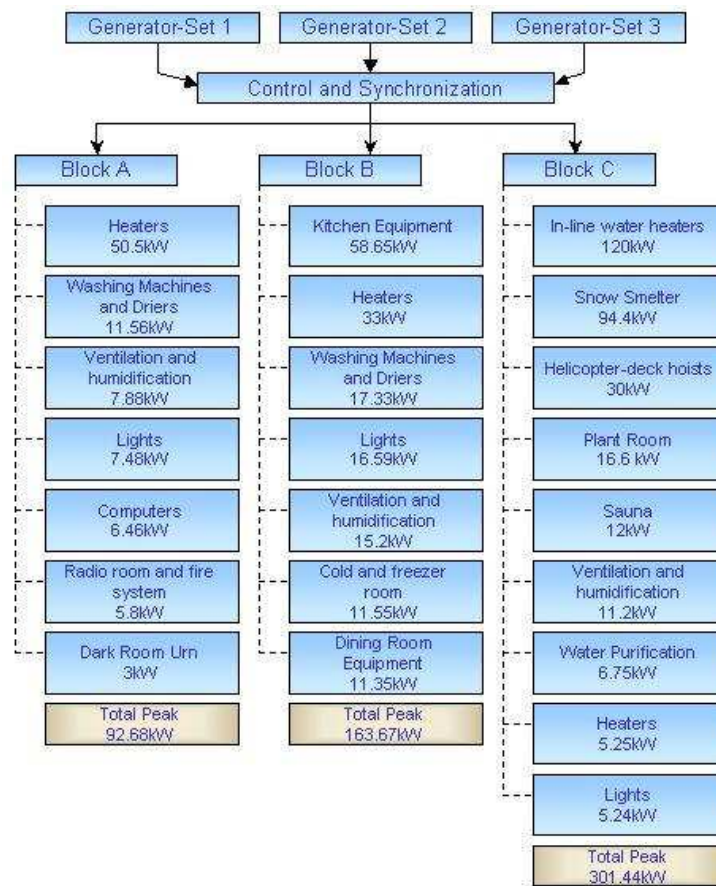


Figure 3.3: Peak power demand breakdown of energy consumers (updated from Tetz, 2002)

Table 3.2: Electricity consumption data, 2005

PARAMETER	TOTAL
Four-Year Average Annual Electricity Consumption (kWh)	1 061 971
Expected Maximum Daily Electricity Consumption (kWh) <sup>W</sup>	5 160
Expected Minimum Daily Electricity Consumption (kWh) <sup>W</sup>	1 440
Average Daily Electricity Consumption (kWh)	2 910
Average Daily Electricity Load (kW)	121.2

<sup>W</sup>Tetz (2002)

Two design aspects of the plant room (which houses the diesel-electric generators) merit further discussion. Firstly, even though one of the three generators is an inter-cooled combustion engine, the fluid used in the intercooler is taken from the Primary Hot Water System (with temperatures often in the region of 90°C). Water supplied from the Domestic Cold Water System would in all

likelihood result in higher engine efficiencies. Secondly, although the station Engineers currently funnel air from a ventilation fan in the plant room (i.e. cold outside air) to the air-intake of the generators, the plant room itself is normally perilously close to its maximum allowable temperature during takeover (Cencelli, 2002). It is suggested that one window in the plant room be replaced with a fan and some flexible tubing so that more cold air can be used where desired during the summer.

Adding renewable electrical energy to the mini-grid of SANAE IV is a feasible option for using solar energy devices. The base energy demand is able to accept large contributions from renewable energy devices without requiring energy storage (refer to figure 3.3), and there exists the associated benefit of reducing the problematic amount of waste heat generated by the diesel-electric generators during the summer months (as discussed in section 3.2.2).

### **3.2.5 PLC System**

The PLC Systems essentially carry control information to and from machinery all around the station. Cencelli (2002) noted that improved operation could be achieved if these PLCs communicated amongst themselves and were not isolated from each other as is currently the case. In particular Cencelli gave the following example. High temperatures inside the station will cause the FCU fans to turn faster (and in so doing blow more cold air into the base) on command of the FCU PLCs. This in turn will result in FCU Water Loop temperatures dropping away from their set-point values. Consequently heat will be added to the FCU Water System (on command of the Main Plant 1 PLC) through in-line heaters that maintain the temperature of the FCU Water System at a pre-determined temperature. This ultimately results in greater diesel consumption, when, in fact, it is not at all necessary. Linking PLCs as recommended could prove to be beneficial. Currently the engineers turn all heating elements off during the takeover period to circumvent many of the difficulties normally encountered during this period.

The electricity consumption of the PLC System is known to be negligibly low. Thus, feeding renewable energy into the power grid is most likely the best method to support this system.

### **3.2.6 Sewage System**

SANAE IV processes all of its own waste. While solid waste is transported back to South Africa the fluids are purified and disposed of locally. Initially the effluent is stored temporarily in two

tanks located inside the links, after which it is pumped to the water purification plant. In total this system draws only about 6.75 kW of electricity, and ss with the PLC System a very flexible solution to supplementing this system’s energy needs would be to simply supply the electrical mini-grid with renewable energy.

### 3.3 Fuel Consumption and Energy Demand

Temperatures at SANAE IV may reach -40°C in the middle of winter. Under these conditions ordinary diesel would freeze, so consequently a Special Antarctic Blend (SAB) is used for powering the energy systems. Table 3.3 below lists some of the properties of this fuel.

Table 3.3: Properties of SAB

PROPERTY	VALUE
Specific Viscosity (N.s/m <sup>2</sup> )	1.4
Density (kg/m <sup>3</sup> )	800
Sulphur Content (% m/m max)	0.1
Freezing Point (°C)	-65
Lower Heating Value (kWh/L)	9.8

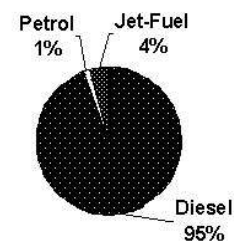


Figure 3.4: Diesel bunker located 400 m from the base (Olivier, 2005)

Details of the annual fuel consumption at SANAE IV are presented below in tables 3.4 and 3.5. The generator diesel consumption is calculated on a four-year average using records from the base (see end of appendix C.5) while the report by Taylor et al. (2002) has been used to obtain the values for the Challenger and Caterpillar D6 Dozer consumption listed in table 3.5. The Skidoo and aeroplane consumption values are rough estimates, and negligibly small amounts of LPG Gas have been omitted from the analysis.

Table 3.4: Average annual fuel consumption by type

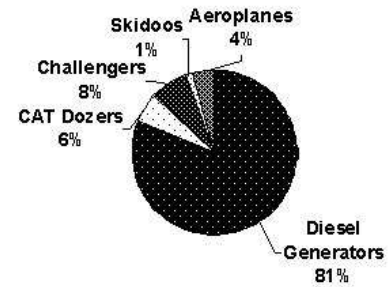
SOURCE	AVERAGE ANNUAL FUEL CONSUMPTION (LITRES)
Diesel	347 222
Petrol <sup>¥</sup>	5 000
Jet-Fuel <sup>¥</sup>	15 000



<sup>¥</sup>Estimated values

Table 3.5: Average annual fuel consumption by user

SOURCE	AVERAGE ANNUAL FUEL CONSUMPTION (LITRES)
Diesel Generators	297 872
CAT Dozers <sup>H</sup>	21 600
Challengers <sup>H</sup>	27 750
Skidoos <sup>Y</sup>	5 000
Aeroplanes <sup>Y</sup>	15 000



<sup>H</sup>Taylor et al. (2002); <sup>Y</sup>Estimated values

It is evident from table 3.5 that due to the large component of diesel in the breakdown of total fuel consumption any time and effort spent optimising the systems that utilise diesel, specifically the diesel generator system, should result in good returns on investment.

Figure 3.5 is a plot of the average monthly generator diesel consumption at SANAE IV that essentially represents the data illustrated in tables 3.4 and 3.5 temporally. An explanation for the three outlying data points of the year 2004 is provided in the discussion below where some important consumption related issues are also investigated.

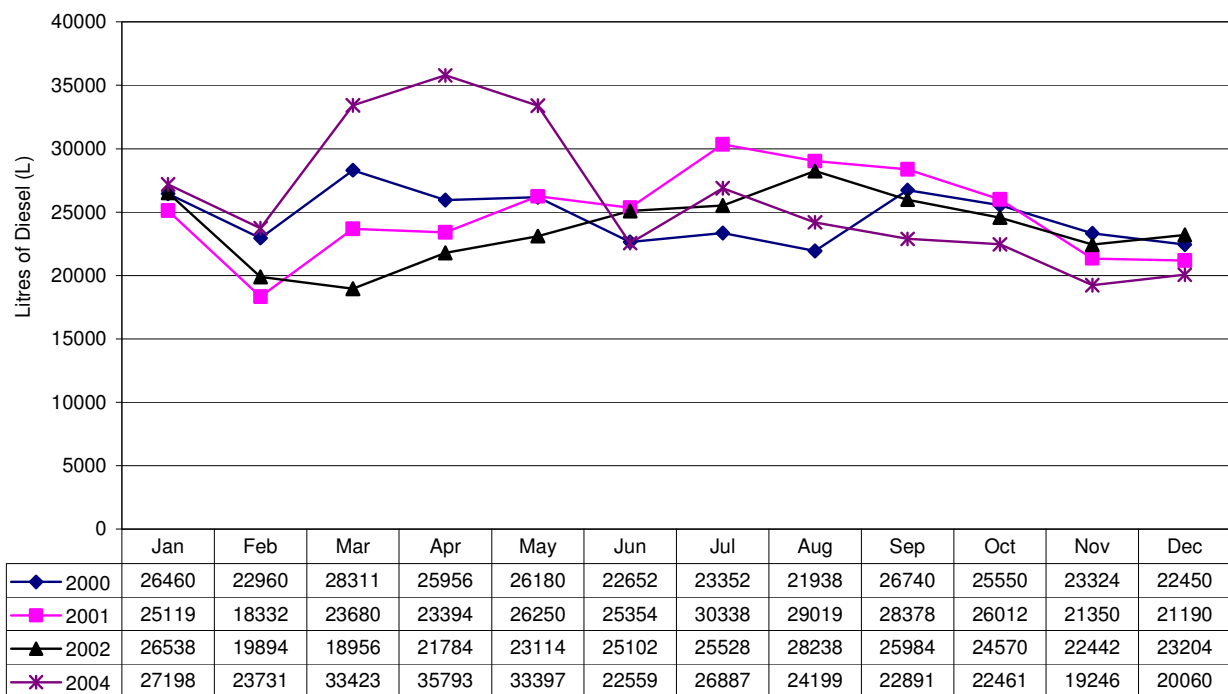


Figure 3.5: Generator diesel usage from the years 2000, 2001, 2002 and 2004

Over the last four years of data collection the average generator diesel consumption has amounted to 24 822 litres per month or 297 872 litres annually. The total monthly consumption remains reasonably constant throughout the year even though the number of people inhabiting the base is reduced from approximately 80 to 10 when comparing takeover to overwintering periods. This energy-demand “inertia” is almost certainly due to the fact that sections of the base are not decommissioned as the number of people residing at SANAE IV changes. Consequently the space of the station that requires heating and ventilation essentially remains the same. From figure 3.3 it is conceivable that decommissioning one Block of the base could result in as much as a 20 % reduction in average generator load, and using equation 3.1 it is found that these energy savings would translate into an annual diesel saving of 18 %. This is a reduction in yearly diesel consumption of 61 595 litres. Unfortunately such changes are not possible to implement since, amongst other problems, the hospital, kitchen and plant room are all located in separate blocks. Infrastructure such as pipes and cabling for instance have also not been designed for this purpose.

It is reasoned that the unprecedented fuel demand shown in figure 3.5 during March, April and May of 2004 was due to an increased heating load in the base caused essentially by ambient conditions. As temperatures drop the base “shrinks”, an effect of colder weather that can cause cracks to open around windows and where the links join onto the main Blocks for instance. Warm air will now escape and locally temperatures inside these areas of the base will plummet. If these cracks are attended to the smaller ones can be sealed with pliable materials such as silicon and remain closed for a number of seasons. The effort undertaken by the overwintering team during June 2004 to find and seal these holes, but especially to minimise the use of heaters, most likely resulted in a reduced consumption from June 2004 onwards. Teetz (2000) estimates that during very cold weather as much as 32 kW of heat is lost through leakages around doors and other seals, which is over a quarter of the annual average electricity demand. Thus, any measures that can be taken to reduce this type of heat loss are encouraged.

### **3.3.1 Temporal Variations of Energy Demand**

An average profile of the monthly generator diesel consumption is plotted in figure 3.6 not including the three outlying data points of March, April and May 2004. According to this figure the effect of seasonal temperature and weather changes are moderate and probably account for a maximum difference of 5100 litres of diesel consumed per month. This is almost equivalent to

the effect of population variations (that is, comparing the summer months with and without takeover crew), which appear to translate into monthly differences of 5700 litres.

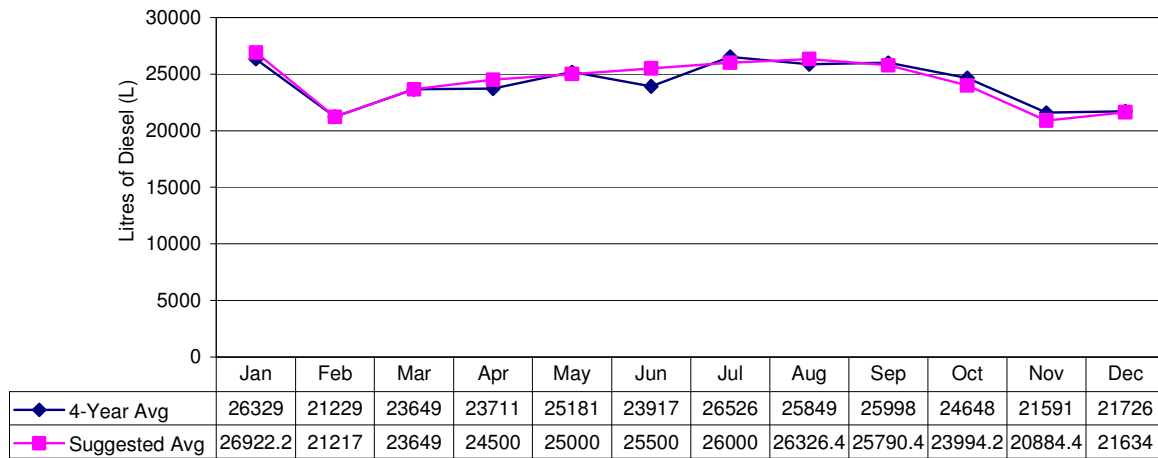


Figure 3.6: Monthly variations of diesel consumption

Comparatively, daily electricity consumption during the summer takeover period is very erratic. Odd maintenance jobs and other projects are carried out around the base at irregular intervals since the long hours of sunlight allow people to work till late at “night” on tasks that would otherwise be postponed to the following day. The result is a load profile that is prone to large daily variations. Using mean values would therefore result in significant mismatches between the demanded energy and that supplied by renewable resources.

A graph of daily station electrical load during the summer takeover period is presented in figure 3.7 (further details are supplied in appendix C.4). The figure shows a load average of 134.7 kW, which is a value that corresponds well with data in table 3.2 and implies that the measurements used to create this graph was not exceedingly far from normal operating conditions. Note, however, that when comparing the 19-day average profile in this figure to a single day’s worth of measurement there is a marked reduction of variability. On average the peaks and troughs of the data used were 28 % above and below their respective means, displaying a significant reduction in load swings.



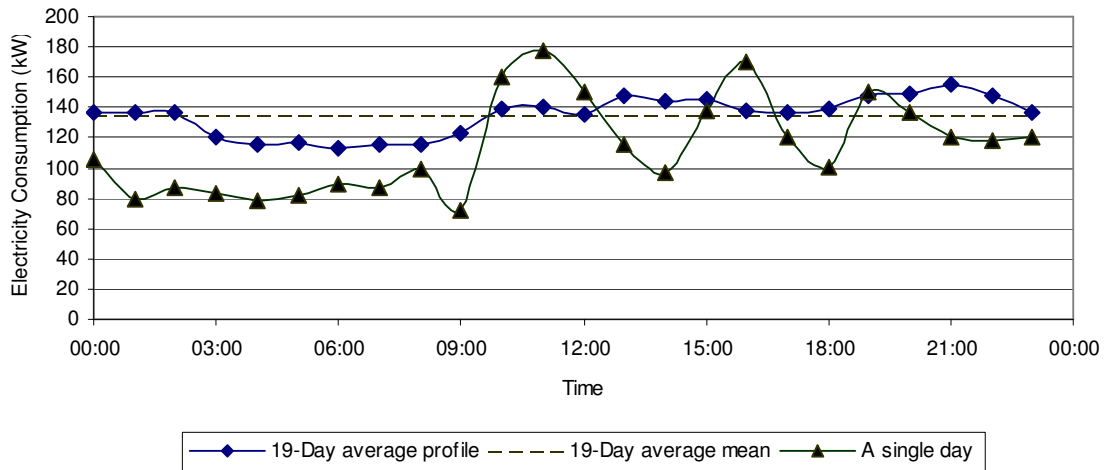


Figure 3.7: Average load profiles

For the purposes of this project the base-load of the station will be used for further investigation (refer to figure 3.8). The implication is that any solar energy supplied to the station will always be met with the expected demand (since this demand should always exceed the base load). Due to the magnitude of the base electrical load at SANAE IV (approximately 60 kW) it is highly unlikely that a renewable energy system will supply beyond this minimum. However, any design that does aim to supply energy somewhere between this minimum and the average value will have to account for those times that available energy will not be utilised.

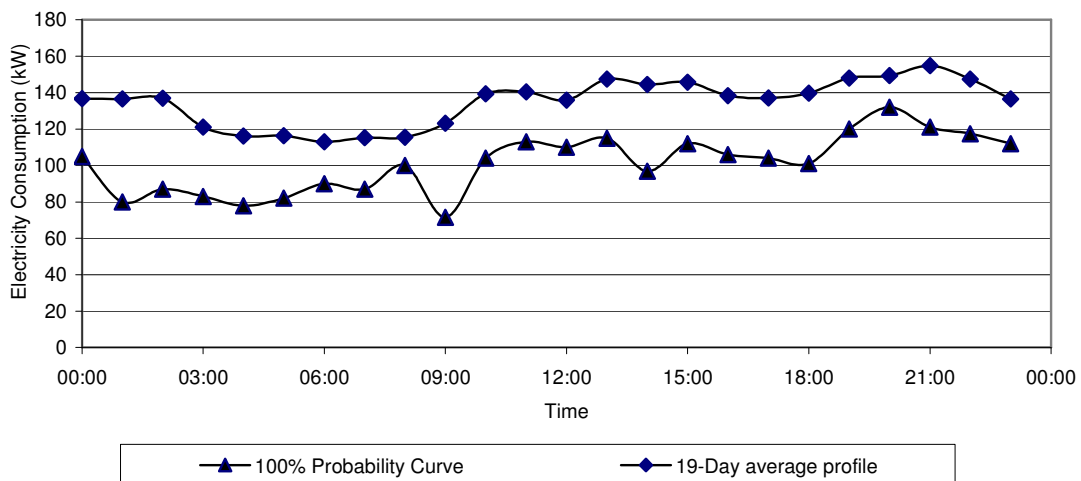


Figure 3.8: Minimum and average generator load profile at SANAE IV

### **3.4 Summary**

The energy systems at SANAE IV have been investigated in chapter 3 by classifying and studying the individual components in detail (refer to figure 3.1). There exists the potential not only to reduce diesel consumption by implementing a solar energy system, but also to increase the station's independence from this fuel source since currently the generators provide 100 % of the station's electrical and thermal needs. The loads best suited to solar energy applications were identified as the SANAE IV electrical mini-grid and snow smelter

Suggestions for possible improvements to some of the station's energy systems were made throughout the chapter. Notably, some of the difficulties with PLC control (c.f. section 3.2.5), plant room temperatures during the summer takeover period (c.f. section 3.2.4), heat losses to the environment (c.f. section 3.3) and the potential for improvements through updating the existing station simulation programme (c.f. section 3.2.3) were discussed.

It is further suggested that an effort is made to implement the changes discussed above before undertaking to install a solar or other renewable energy device. The large amounts of capital and effort that will go into commissioning a renewable energy system at SANAE IV could best be justified if firstly, the station is not wasting or poorly utilising energy, and secondly, all of the most significant shortcomings have already been addressed (i.e. Pareto's Principle).

# Chapter 4 – Solar Energy Capturing Solutions

## 4.1 Introduction

Figure 4.1 below illustrates some of the processes that solar radiation will undergo before it can be used at the station. Since the available solar insolation throughout the year has already been estimated in chapter 2, and the energy demand of South Africa’s base was studied in chapter 3, it remains in this chapter only to investigate the characteristics of the individual solar energy devices.

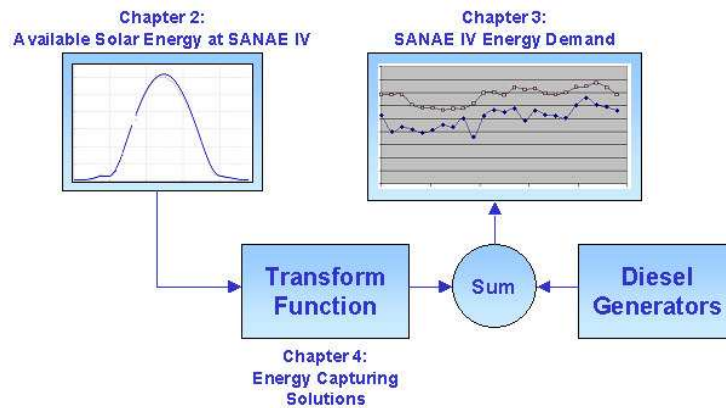


Figure 4.1: SANAE IV solar energy system

Solar-energy devices may be classified as either electrical or thermal collectors. Ordinarily electrical collectors (i.e. photovoltaic or PV panels) are easier to commission, however they also have significantly lower system efficiencies traditionally in the order of 10 %. Conversely solar thermal devices may collect as much as 75 % of the available solar radiation, yet this value is highly dependent on ambient temperatures and radiation levels. The final product of hot water or steam produced by solar thermal devices may also be of little use if there are no thermal loads. In this instance it is therefore necessary to compare the various alternatives of capturing solar energy by considering more carefully the conditions relevant to SANAE IV.

Chapter 4 calculates expected performance characteristics of various solar energy systems at SANAE IV. It begins with a brief overview of the solar energy industry, and then investigates PV and solar thermal systems respectively for the given conditions. The expected efficiencies of recommended photovoltaic and solar thermal collectors have been calculated in sections 4.2.3 and 4.3.1, and the relevant energy savings summarised in tables 4.6 and 4.9. The reader is also referred to appendix D for supplementary information.

## 4.2 Solar Electric Collectors

### 4.2.1 Background

Solar electric technology has developed tremendously since its inception in 1954 when it was first used in the space industry yet has never become a large-scale contributor of global energy demand (Yates, 2003). Even though certain photovoltaic cells can harness up to 36 % of the available insolation (produced by Spectrolab, a subsidiary of Boeing) this top-end technology is not currently economically feasible and traditional efficiencies of 11 to 15 % are more common. There is a general misconception concerning solar panels and wind turbines, which suggests that it requires more energy to manufacture these devices than what they will produce in their lifetime (Corkish, 1997). The *energy payback* periods for solar PV panels are normally six years, while their average lifetimes may exceed twenty-five years.

Conventional PV systems are ideally suited for low wattage electrical loads at isolated locations where the cost of laying power-lines far exceeds the cost of newly installed panels. In these instances (e.g. radio repeater stations, borehole water-pumping, ocean buoy lights etc.) the benefits of utilising solar energy far outweigh the associated costs, yet the growing PV market is also being fuelled by installations meant as a means of generating large-scale energy supplies (refer to figure 4.2). Such photovoltaic deployment remains expensive, however, even when considering environmental costs. The PV marker in figure 4.3 for instance is not shown, lying at a distant [0.88 US\$/kWh, 22 000 US\$/kW] according to Broniki (2001) (also consult Helm [2005]).

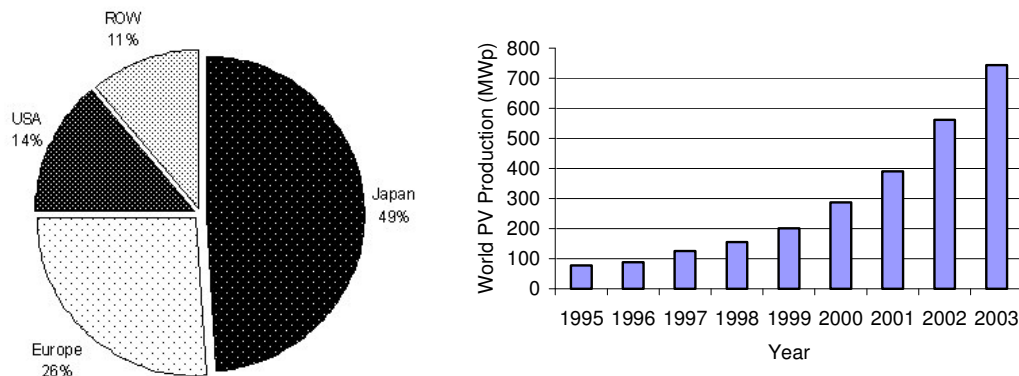


Figure 4.2: Apportioned photovoltaic production in 2003, and historical trend (EPIA, 2005)

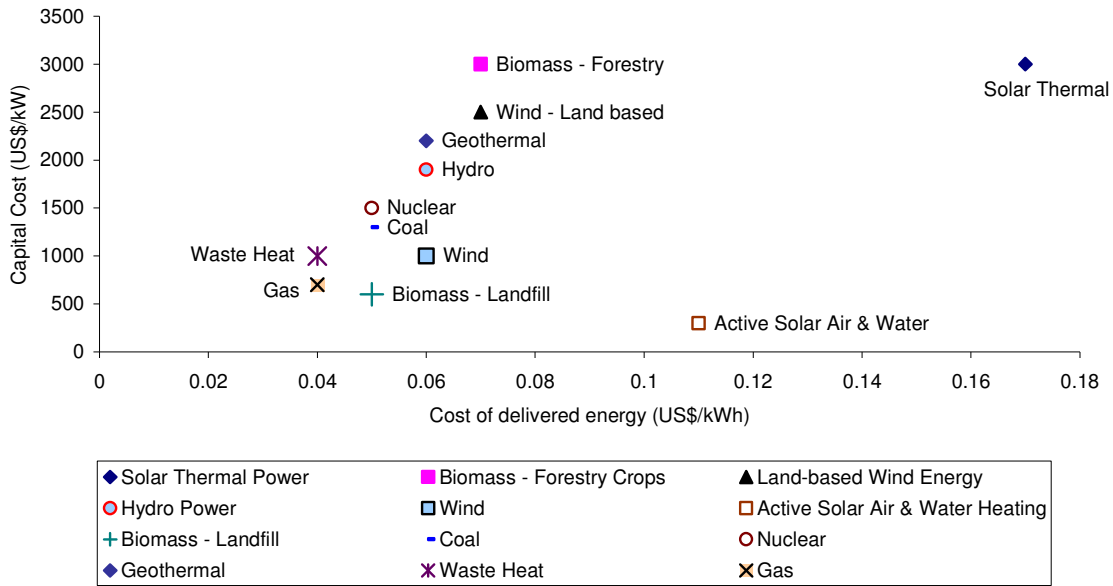


Figure 4.3: Costs of renewable and other energy generation methods (Broniki, 2001)

Nonetheless, photovoltaic panels will play an increasingly important role in power generation. This should occur as greater emphasis is placed on environmental concerns, increased global demand for oil hinders the *availability* of conventional fossil fuels (and not initially the total reserves remaining [Helm, 2005]) and possibly as the costs of PV panels are further reduced by the economy of scale and technological advances as shown in figure 4.4. PV systems offer a clean, reliable and sustainable source of energy that is bound to establish itself in various niches of the energy market.

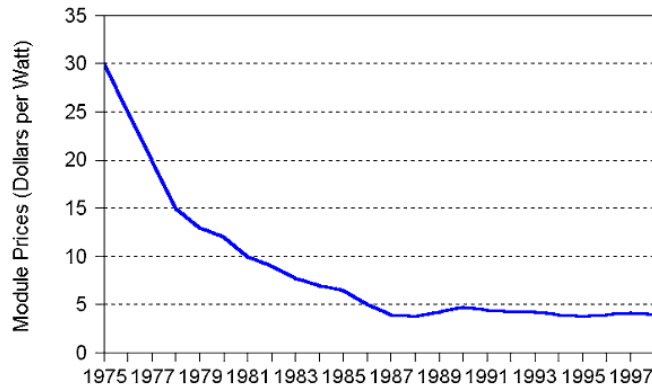


Figure 4.4: Photovoltaic prices from 1975 to 1998 (Maycock, 1999)

## 4.2.2 Implementing Photovoltaics at SANAE IV

The relatively large 60 kW base-load at SANAE IV (refer to section 3.3.1) allows substantial contributions to be made by a photovoltaic system without incorporating the use of storage devices. Any electrical supply larger than this base-load would require the use of batteries, allowing for greater energy contributions but also increasing the energy generation costs in R/kWh. In view of the economic results given in section 5.8.1 this would make a photovoltaic system completely economically unfeasible for use at SANAE IV. Consequently energy storage devices have not been included in the ensuing investigation of PV systems and consideration has only been given to the solar panels, Maximum Point Power Trackers or MPPTs (that maximise the photovoltaic output at all light conditions) and inverters (that convert direct current [DC] to alternating current [AC]).

A more detailed representation of the suggested photovoltaic system for use at SANAE IV is presented in figure 4.5. It is acceptable to assume that the inverter and MPPT have transform functions that can be modelled by simple constants (efficiencies of above 90 %) and will allow estimates of panel efficiencies to be obtained in section 4.2.3.

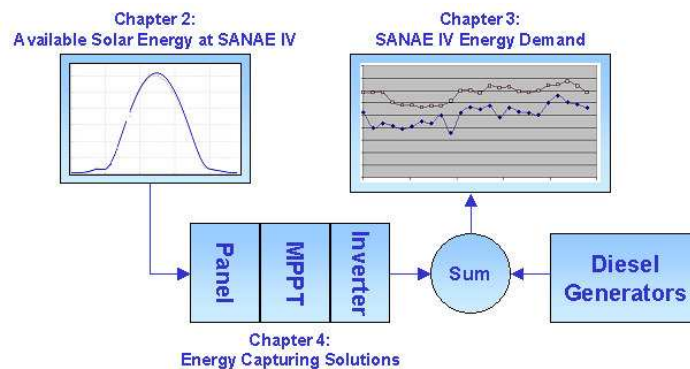


Figure 4.5: SANAE IV solar energy system implementing photovoltaic panels

## 4.2.3 Expected Efficiencies of Photovoltaic Panels at SANAE IV

South Africa does not currently manufacture any of its own solar panels. All photovoltaic cells are purchased from overseas' manufacturers as either ready for re-sale in the module form, or ready for final assembly. For the purpose of this investigation three local South African companies that stock photovoltaic panels were sourced, the results of which are presented below.

Table 4.1: Local South African suppliers of photovoltaic panels

	KYOSERA	SANYO	SHELL	TOTAL ENERGY
Solardome	✓	✓	✓	×
Solar Power Products	×	×	✓	✓
SINETECH	×	✓	✓	×
Nominal Efficiency	15 %	15 %	13 %	11 %

Commercially available photovoltaic panels are categorised according to the atomic structure of the photovoltaic material, viz. mono-crystalline, poly-crystalline, thin-film etc. (refer to figure 4.6 below). The atomic structure in turn is determined by the manufacturing process of the panel and is consequently very closely related to the final cost. Panel efficiency will generally increase with an increasing order in the atomic structure; yet it will also become harder to manufacture the panel and thus the more expensive it will be to purchase.

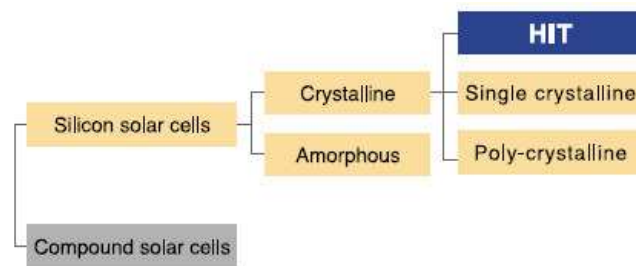


Figure 4.6: Breakdown of available solar technology (SANYO, 2005)

Mono-crystalline photovoltaic cells are generally slightly more efficient than their poly-crystalline counterparts (15-18 % and 10-14 % respectively), while amorphous cell efficiencies range between 6-7 % and exhibit shorter lifetimes (Yates, 2003). Amorphous cells are much cheaper to manufacture, yet for the reasons given above they are not commonly utilised in large systems except when initial cost is an inhibiting factor. In figure 4.6 the relatively new technology of Heterojunction with Intrinsic Thin layer (HIT) SANYO panels is also specified which show efficiencies and costs very similar to the mono-crystalline cells.

#### JANUARY EFFICIENCY ESTIMATES USING MANUFACTURER SPECIFICATIONS

Nominal efficiencies are often provided for photovoltaic panels by manufacturers, specified at the Standard Testing Conditions (STC) of 1000 W/m<sup>2</sup> illumination and a cell temperature 25°C. Using the widely accepted temperature dependence of 0.5 %/°C (Yates, 2003) for photovoltaic

panels and the average measured PV cell temperature at SANAE IV during January of 1°C (refer to section 2.3.1) the expected efficiency of a photovoltaic panel at SANAE IV can be calculated using:

$$\eta_{total} = \left( \frac{P_o (1 + \eta_{temp} \times [T_{STC} - T_{cell}])}{P_i} \right) \times \eta_{losses} \quad 4.1$$

Where  $P_i$  is the available solar radiation (W),  $P_o$  is the output power at the nominal maximum power point (W),  $\eta_{temp}$  is specified as 0.5 %/°C,  $T$  is temperature (at STC and actual cell operating conditions respectively, in °C) and  $\eta_{losses}$  is the combined efficiency of the ancillary equipment (estimated as 93 % for a MPPT and 96 % for an inverter). Some results for the standard PV collectors defined in section 4.2.3 have been presented in table 4.2.

Table 4.2: Expected January efficiencies at ambient SANAE IV conditions

PV TYPE	CELL TEMP (°C)	NOMINAL EFFICIENCY (%)	TOTAL EFFICIENCY (%)	TILTED YIELD (kWh/m <sup>2</sup> .day)
Mono-crystalline	1	15	15.12	1.22
Poly-crystalline	1	11-14	11.08-14.11	0.85-1.14
Thin film	1	6-7	6.04-7.06	0.49-0.57

#### JANUARY EFFICIENCY ESTIMATES USING HEAT TRANSFER CALCULATIONS

A second method of estimating the efficiencies at a given set of ambient conditions is presented by Yates (2003). Here a heat transfer analysis is carried out on a solar panel assuming that the thermal characteristics of the panel are known (such as thermal resistance). Although this method is rigorous the values used in this investigation are broad averages and, consequently, calculated answers will differ somewhat from values of specific PV panels. The process is most useful if the true properties (that are measurable although unfortunately not often specified by manufacturers) of the panel in question are known. The equation used is:

$$P_c = \frac{P_i(1 - \alpha)(1 - \mu_T R_T(1 - \alpha)P_i)}{1/\eta_N - \mu_T R_T(1 - \alpha)P_i} - P_{losses} \quad 4.2$$



Where  $P_c$  is the collected radiation ( $\text{W/m}^2$ ),  $P_i$  is the incident radiation ( $\text{W/m}^2$ ),  $\alpha$  is the reflectivity of the collector cover,  $\mu_T$  is the percentage decrease in efficiency with increased temperature ( $\%/^\circ\text{C}$ ),  $\eta_N$  is the nominal efficiency and  $R_T$  is the thermal resistance ( $\text{K.m}^2/\text{W}$ ). The power losses  $P_{\text{losses}}$  are assumed to be due to a charge controller (viz. a MPPT and inverter combined) operating at an average efficiency of 90 %. Hence, using standard values of  $\alpha = 0.06$ ,  $\mu_T = 0.004$ ,  $R_T = 1.95$  and  $\eta_N$  given individually in table 4.3 total efficiencies and estimated yields can be provided. The results are also shown in table 4.3.

Table 4.3: Heat transfer analysis of photovoltaic panels

PV TYPE	NOMINAL EFFICIENCY (%)	TOTAL EFFICIENCY (%)	TILTED YIELD ( $\text{kWh/m}^2.\text{day}$ )
Mono-crystalline	15	12.69	1.02
Poly-crystalline	11-14	9.30-11.84	0.75-0.96
Thin film	6-7	5.07-5.92	0.41-0.48

#### JANUARY EFFICIENCY ESTIMATES USING RETSCREEN

A third technique used to compare the efficiencies of photovoltaic panels is the methodology presented by RETScreen (RETScreen, 2005). This organisation, which is supported by the United Nations Environment Programme (UNEP), NASA and the Global Environment Facility (GEF), “...seeks to build the capacity of planners, decision-makers and industry to implement renewable energy and energy efficiency projects”, and suggests that the procedure shown in figure 4.7 be used to determine efficiencies of PV systems at non-standard conditions.

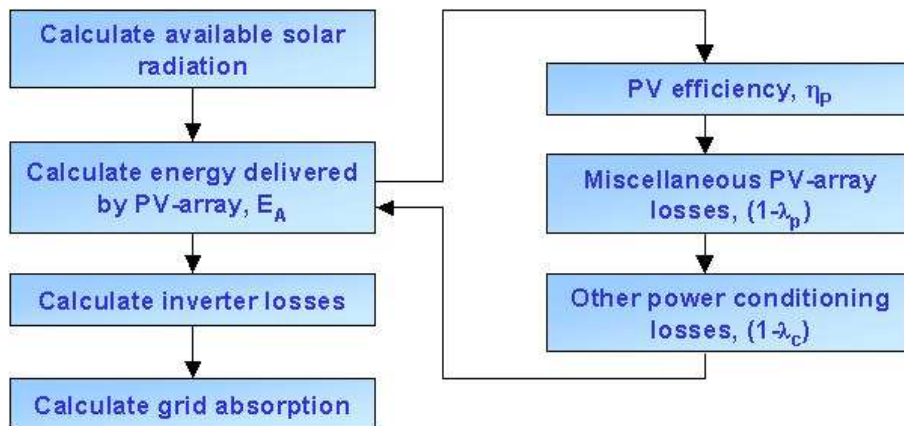


Figure 4.7: RETScreen On-Grid Energy Model flowchart

Referring to figure 4.7 the following associated equations and information are provided by RETScreen:

$$\eta_p = \eta_r \cdot (1 - \beta_p(T_c - T_r)) \quad 4.3$$

$$T_c = T_a + (219 + 832 \cdot K_t) \left( \frac{NOCT - 20}{800} \right) \quad 4.4$$

$$E_A = E_p \cdot (1 - \lambda_p)(1 - \lambda_c) \quad 4.5$$

$$E_p = A \cdot \eta_p \cdot H_t \quad 4.6$$

$$\eta_A = \frac{E_A}{A \cdot H_t} \quad 4.7$$

Here  $\eta_A$  is the total array efficiency and  $\eta_p$  is the efficiency of a single panel. The symbol  $A$  is the surface area of the array ( $m^2$ ),  $H_t$  is the solar insolation at the specified location ( $kWh/m^2$ ),  $E_A$  is the array energy available for use ( $kWh/m^2$ ),  $E_p$  is the energy delivered by the PV array ( $kWh$ ),  $\lambda_p$  are the “*miscellaneous PV array losses*” (in this instance equal to 0),  $\lambda_c$  are the “*other power conditioning losses*” (estimated at 0.07 for the MPPT),  $K_t$  is the clearness index (estimated as 0.65 for January [refer to section 2.3.3]),  $NOCT$  is the Nominal Operating Cell Temperature ( $^{\circ}C$ ),  $T_a$  is the ambient temperature ( $^{\circ}C$ ),  $T_c$  is the average module temperature ( $^{\circ}C$ ),  $T_r$  is the reference temperature ( $25^{\circ}C$ ),  $\beta_p$  is the temperature coefficient of module efficiency ( $\%/^{\circ}C$ ), and  $\eta_r$  is the PV module efficiency at reference room temperature. In this instance the inverter losses are assumed to be 4 % and the electrical mini-grid absorption losses are taken to be equal to 0 %.

Table 4.4: PV module characteristics for standard technologies (RETScreen, 2005)

PV MODULE TYPE	$\eta_r$ (%)	<i>NOCT</i> (°C)	$\beta_p$ (%/°C)
Mono-Si	13.0	45	0.40
Poly-Si	11.0	45	0.40
a-Si	5.0	50	0.11
CdTe	7.0	46	0.24
CIS	7.5	47	0.46

Table 4.5: RETScreen analysis of PV panels (using equations 4.3 – 4.7 and inverter efficiencies)

PHOTOVOLTAIC CELL	NOMINAL EFFICIENCY (%)	TOTAL EFFICIENCY (%)	TILTED YIELD (kWh/m <sup>2</sup> .day)
Mono-crystalline	15	13.81	1.11
Poly-crystalline	11-14	10.13-12.89	0.82-1.04
Thin film	6-7	5.53-6.45	0.45-0.52

#### COMPARISON OF EFFICIENCY ESTIMATES

The methodology presented by RETScreen will be used as the benchmark of further investigation. Using equations 4.3 to 4.7 the annual averages of the expected amounts of energy that could be captured with solar electric devices have been calculated, and are presented in table 4.6.

Table 4.6: Expected efficiencies and daily energy capture from different PV materials

			MONO-CRYSTALLINE		POLY-CRYSTALLINE		THIN FILM	
	<i>Average Temp</i> (°C)	<i>kWh/m<sup>2</sup></i> <i>Available</i>	<i>Average</i> <i>Efficiency</i>	<i>kWh/m<sup>2</sup></i> <i>Captured</i>	<i>Average</i> <i>Efficiency</i>	<i>kWh/m<sup>2</sup></i> <i>Captured</i>	<i>Average</i> <i>Efficiency</i>	<i>kWh/m<sup>2</sup></i> <i>Captured</i>
January	-6.60	8.05	13.81	1.11	11.51	0.93	5.99	0.48
February	-10.30	6.11	14.01	0.86	11.68	0.71	6.07	0.37
March	-14.90	3.51	14.26	0.50	11.88	0.42	6.18	0.22
April	-18.20	2.54	14.43	0.37	12.03	0.31	6.25	0.16
May	-19.50	0.01	14.50	0.00	12.09	0.00	6.29	0.00
June	-20.10	0.00	14.54	0.00	12.11	0.00	6.30	0.00
July	-23.10	0.00	14.70	0.00	12.25	0.00	6.37	0.00
August	-22.90	1.24	14.69	0.18	12.24	0.15	6.36	0.08
September	-22.90	3.23	14.69	0.47	12.24	0.40	6.36	0.21
October	-18.20	6.86	14.43	0.99	12.03	0.83	6.25	0.43
November	-12.80	7.14	14.14	1.01	11.79	0.84	6.13	0.44
December	-7.10	8.30	13.84	1.15	11.53	0.96	6.00	0.50
<b>Average</b>	<b>-16.40</b>	<b>3.92</b>	<b>14.34</b>	<b>0.56</b>	<b>11.95</b>	<b>0.47</b>	<b>6.21</b>	<b>0.24</b>

It should be noted that research conducted by the AAD (which has installed two solar energy systems at stations on the continent) established that tilted collectors, as opposed to tracking collectors, are the most economical solution for harnessing solar energy in Antarctica (AAD, 2005). The AAD determined that collectors tilted towards the sun collected greater amounts of solar energy justifiable in view of the added cost, however the same was not true for tracking collectors.

### 4.3 Solar Thermal Collectors

The types of solar thermal systems that could potentially be implemented at SANAE IV range from the standard flat-plate collectors to high-temperature concentrating devices. As an instructive tool for evaluating which solar thermal collector might best be suited to the conditions at the South African station a list of all the energy systems currently in use at the various stations in Antarctica has been given in table 4.7 (COMNAP, 2005). This table will be considered shortly below.

Table 4.7: Currently installed renewable energy systems in Antarctica (COMNAP, 2005)

NATION	STATION	TYPE	SIZE	kWh/YEAR
Argentina	Belagrano I	Wind	Not known	Not known
Argentina	Esperanza	Wind	Not known	Not known
Argentina	Primavera	Wind	Not known	Not known
Argentina	San Martin	Wind	Not known	Not known
<i>Australia</i>	<i>Davis</i>	<i>Flat Plate Collector</i>	<i>12m<sup>2</sup></i>	<i>Not known</i>
<i>Australia</i>	<i>Law Base</i>	<i>Photovoltaics</i>	<i>0.4m<sup>2</sup></i>	<i>Not known</i>
Australia	Casey	Wind	Not known	10780 kWh
Australia	Mawson	Wind	2	1288342 kWh
Germany	Neumeyer	Wind	1	Not known
India	Maitri	Wind	Not known	Not known
<i>Japan</i>	<i>Syowa</i>	<i>Photovoltaics</i>	<i>323m<sup>2</sup></i>	<i>40060 kWh</i>
Japan	Syowa	Wind	Not known	22400 kWh
<i>Spain</i>	<i>Juan Carlos I</i>	<i>Photovoltaics</i>	<i>27m<sup>2</sup></i>	<i>Not known</i>
Spain	Juan Carlos I	Wind	3	3641 kWh
<i>Sweden</i>	<i>Wasa</i>	<i>Photovoltaics</i>	<i>20.6m<sup>2</sup></i>	<i>Not known</i>
<i>USA</i>	<i>McMurdo</i>	<i>Photovoltaics</i>	<i>236m<sup>2</sup></i>	<i>2390 kWh</i>
USA	McMurdo	Wind	Not known	8930 kWh

From table 4.7 it is evident that by far the most popular renewable energy systems currently installed are wind turbines since eleven out of the seventeen stations cited above are currently using this resource (viz. Argentina, Australia, Germany, India, Japan, Spain and the USA). Next to wind the solar-electric devices are the second most popular energy devices, with Japan and America both having commissioned large photovoltaic plants (in excess of 300 and 200 square-meters respectively). The solar energy systems of Australia, Spain and Sweden are much more moderately sized however. There is also a single flat-plate solar collector installed at Australia's Davis station which "...perform[ed] very satisfactorily", and could produce hot water at a cost "...comparable to, if not lower than diesel", (Antarctic Renewable Energy, 2005).

Since Antarctica is widely known as the windiest place on Earth it is not surprising that a fair number of wind turbines have been installed on the continent. These devices can sometimes operate competitively with local and conventional electricity generation methods (refer to figure 4.3), while comparatively electricity generation in Antarctica is subject to the added difficulty of transporting fuel to remote stations. Wind is also available throughout the year and not subject to

large seasonal variations of availability providing this resource with a fair competitive edge over solar energy.

The usefulness of solar energy in Antarctica seems questionable in comparison since only for a short period in the summer is there an abundance of solar radiation, and because on average insolation rates are low ( $3.92 \text{ kWh/m}^2 \cdot \text{day}$  annual average insolation at SANAE IV). There are currently only two large PV installations in Antarctica (out of 17 installed renewable energy systems) aimed at significant displacement of diesel. These systems are also never found preceding the installation of a wind turbine. Nonetheless, the difficulty and cost involved in transporting fuel to stations should make this energy generation method desirable in some instances.

Yet, from table 4.7 the potential for utilising solar thermal devices before wind turbines or photovoltaic panels seems doubtful. The following section presents an investigation of how solar thermal devices are expected to perform at SANAE IV, and the energy savings that should be generated from such systems.

#### **4.3.1 Selection of a Solar Thermal Collector**

A number of criteria were considered in the selection of a solar thermal device. For instance, from the investigation in chapter 2 it was found that the diffuse fraction of radiation incident at SANAE IV is extremely high. In fact there is only  $2.04 \text{ kWh/m}^2 \cdot \text{day}$  of beam radiation available on average throughout the year to a non-tracking optimally tilted surface in comparison to the  $3.92 \text{ kWh/m}^2 \cdot \text{day}$  of global insolation available to flat-plate collectors. Thus more than half of the average global radiation is diffuse. Ambient temperatures were also considered, and it should be noted that operating temperatures of flat-plate solar thermal collectors will be far lower than concentrating devices; an important consideration for conditions where energy losses to the cold surroundings are already high even at relatively low process temperatures. The marked difficulties in installing the “...*complicated drive system* ...[with] *high energy requirement*” (Tamm, 2005) required for concentrating systems are also a concern, especially since extremely strong winds (often gusting at more than  $120 \text{ km/hr}$ ) common at SANAE IV could most likely damage such a system and probably also cause misalignments and vibrations that resulted in the noticeable efficiency reductions at Eskom’s Stirling Dish test facility in South Africa (van Heerden, 2003).

Therefore a simple and convenient solar thermal device is the flat-plate solar collector. This collector will not only operate at lower process temperatures, but will also be: less susceptible to wind related efficiency losses, more resistant to wind related damage, utilise both the beam and diffuse components of radiation, allow for easier maintenance, and is readily available locally.



Figure 4.8: The solar thermal system installed at Australia's Davis station (AAD, 2005)

#### FLAT PLATE SOLAR COLLECTORS

Three products sourced from companies in South Africa and the United States of America were investigated to estimate probable efficiencies of solar thermal collectors at SANAE IV. Solahart, an Australian based company, manufactures two of these three products (the Bt and Mt collectors) and is not only a supplier to South Africa but also currently the only company to have installed a solar thermal product in Antarctica (see figures 4.8 and 4.14). The second company, Thermomax, is a manufacturer of solar thermal vacuum tube collectors and will be used for comparative purposes. The products manufactured by Thermomax are not readily available in South Africa and require packaging and shipment from overseas.

The performance characteristics of the Solahart and Thermomax products are presented in figure 4.9 (also refer to appendix D.3 to D.5), while figure 4.10 illustrates how the suggested solar thermal system will be incorporated into the current diesel only electricity generation system.

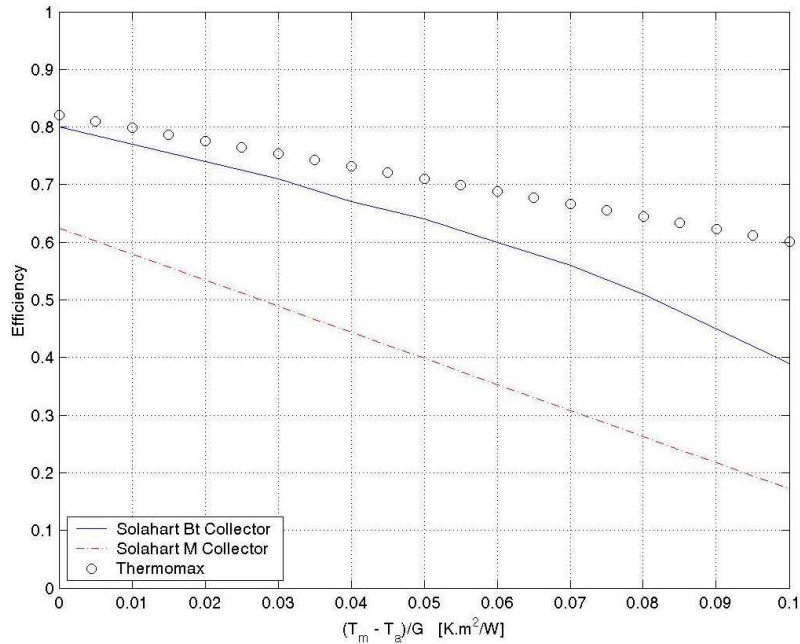


Figure 4.9: Efficiencies of three available flat-plate solar thermal collectors

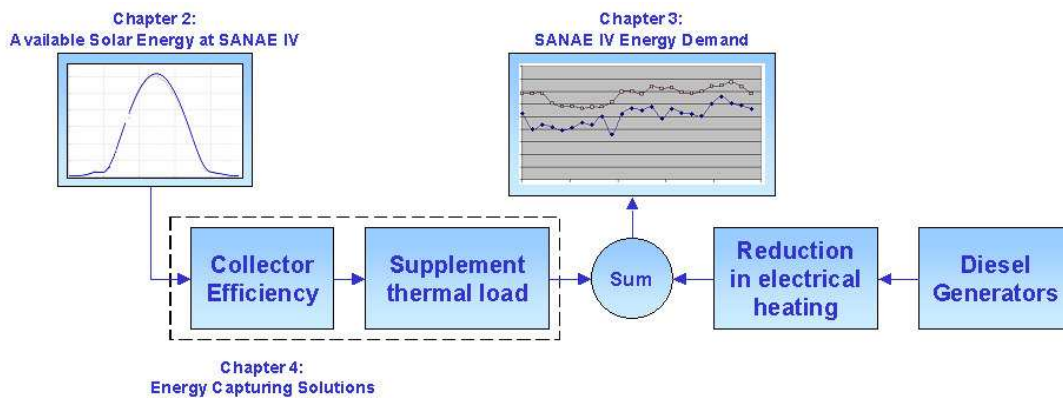


Figure 4.10: SANAE IV solar energy system implementing solar thermal collectors

Of all the thermal loads at SANAE IV the snow smelter was identified in chapter 3 as the most appropriate for supplementing with solar energy. Mainly this was due to the fact that summer H&V loads at the station are negative (implying that the base requires cooling and no contributions from a solar thermal device) and because the Primary Hot Water System already plays an important role in cooling the generators during the summer (and therefore has no use for excess heat, refer to chapter 3). The most significant remaining thermal load, the snow smelter, is not only the cause of excessive generator power consumption, but also a good load to supplement in order to generate greater amounts of fresh-water during the summer takeover period (as explained in section 3.2.2).



To assist in this investigation a simulation programme of the snow smelter operation was created with Matlab V6.1 code using the already existent PLC logic (see appendix D.2 to D.6) and the efficiency curves of the products presented in figure 4.9. In this manner various parameters within the system could be altered (such as collector tilt angle, insolation rate, overall heat transfer coefficient of the heat exchanger, size of the thermal store etc.) and the contribution of the solar thermal collector was analysed.

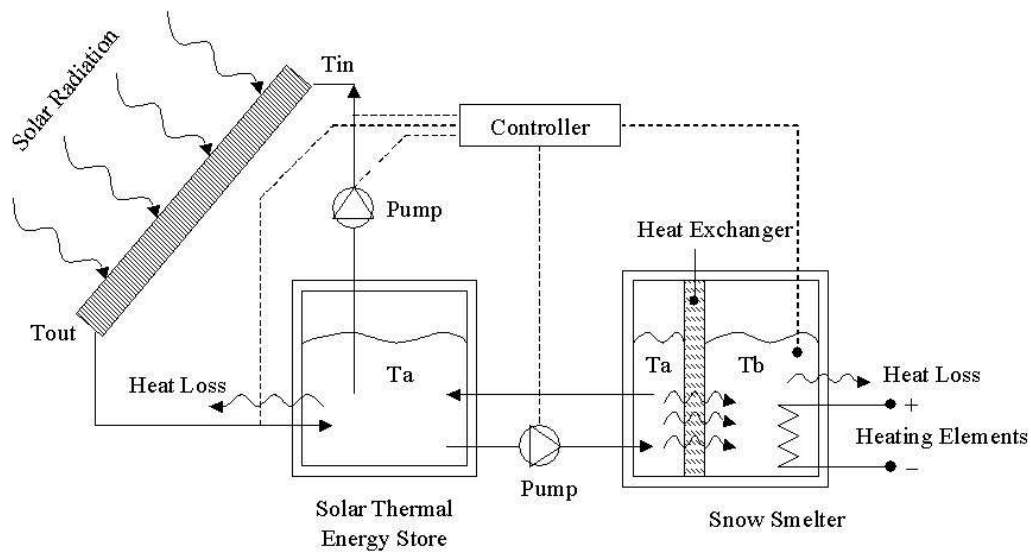


Figure 4.11: Physical connection of solar thermal collector to snow smelter system

Figure 4.11 shows the recommended split solar system, with a solar thermal energy storage tank added to the current snow smelter set-up. The fluid circulating through the thermal energy store and the collector contains anti-freeze (isolated from the main snow smelter), and the collected energy is transferred to the snow smelter's cold-side through a heat exchanger. Pumps are controlled by a PLC and activated such as to prevent either the transfer of heat to the environment through the collector or the transfer of heat from the snow smelter to the energy store. The programme's logic and sample results are presented in figures 4.12 and 4.13, and estimated savings for the Bt collector have been tabulated in tables 4.8 and 4.9. Refer to appendix D.7 for values relating to the Mt and Thermomax collectors.